Supplementary Information for

Ultra-stable all-solid-state perfluoropolyether-based electrolytes for sodium-metal batteries

Dr. X. Wang, Dr. F. Chen, Dr. T. C. Mendes, Prof. P. C. Howlett,

Prof. M. Forsyth

Institute for Frontier Materials (IFM)

Deakin University

Geelong, VIC 3217, Australia.

E-mail: xiaoen.wang@deakin.edu.au; maria.forsyth@deakin.edu.au

Dr. C. Zhang, Dr. C. Fu, Prof A. K. Whittaker

ARC Centre of Excellence in Convergent Bio-Nano Science and Technology and Australian Institute for Bioengineering and Nanotechnology

The University of Queensland

Brisbane, QLD 4072, Australia

E-mail: c.zhang3@uq.edu.au; a.whittaker@uq.edu.au

Dr. Q. Yuan, Prof. D. J. Searles

Australian Institute for Bioengineering and Nanotechnology

The University of Queensland

Brisbane, QLD 4072, Australia

Prof. D. J. Searles

School of Chemistry and Molecular Biosciences and Centre for Theoretical and Computational Molecular Science

The University of Queensland

Brisbane, Queensland 4072, Australia

Dr. Q. Yuan

State Key Laboratory of Precision Spectroscopy

School of Physics and Material Science

East China Normal University

Shanghai 200062, P. R. China

M. Sawczyk, Prof. P. Król

Department of Chemistry and Department of Physics, University of Illinois at Chicago, Chicago, Illinois 60607, United States

Department of Biopharmaceutical Sciences, University of Illinois at Chicago, Chicago, Illinois 60612, United States

Prof. C. J. Hawker

Materials Research Laboratory, Department of Materials, and Department of Chemistry and Biochemistry

University of California, Santa Barbara

California 93106, United States

Table S1. The characterization data of EO-PFPE and EO-CTRL prepared in the study.

polymers[a]	DP_{PEGA}[b]	$M_{n,PEGA}$ (g/mol)[b]	$M_{n,PFPE}$ (g/mol)	$M_{n,BCP}$ (g/mol)[b]	$Đ$[c]	N[d]	f_{PFPE} (%)[e]	T_{ODT} (°C)[f]
EO5-PFPE	5	2000	1400	3600	1.06	37	29.6	113
EO10-PFPE	10	4800	1400	6400	1.20	73	14.9	112
EO20-PFPE	20	9600	1400	11200	1.19	135	8.1	62
EO40-PFPE	38	18000	1400	19600	1.12	243	4.5	-
EO10-CTRL	10	4800	-	4800	1.08	-	0	-

[a]Samples are referred to as EOm-PFPE and EOm-CTRL where m specifies the degree of polymerization of PEGA. [b]Degree of polymerization and number-average molar mass (g/mol) from ^{1}H NMR analysis. [c]Molar mass dispersity of block copolymer from size-exclusion chromatography (SEC) analysis in THF. [d]Volumetric degree of polymerization based on measured homopolymer densities (1.12 and 1.9 g/cm^3 for PEG and PFPE, respectively) at 25 °C and a reference volume, ν, of 118 Å^3. [e]Volume fraction of F based on measured homopolymer densities at 25 °C and ^{1}H NMR. [f]Order–disorder transition temperature (T_{ODT}) in °C determined from dynamic mechanical thermal analysis (DMTA) performed on heating at a rate of 1–2 °C/min.

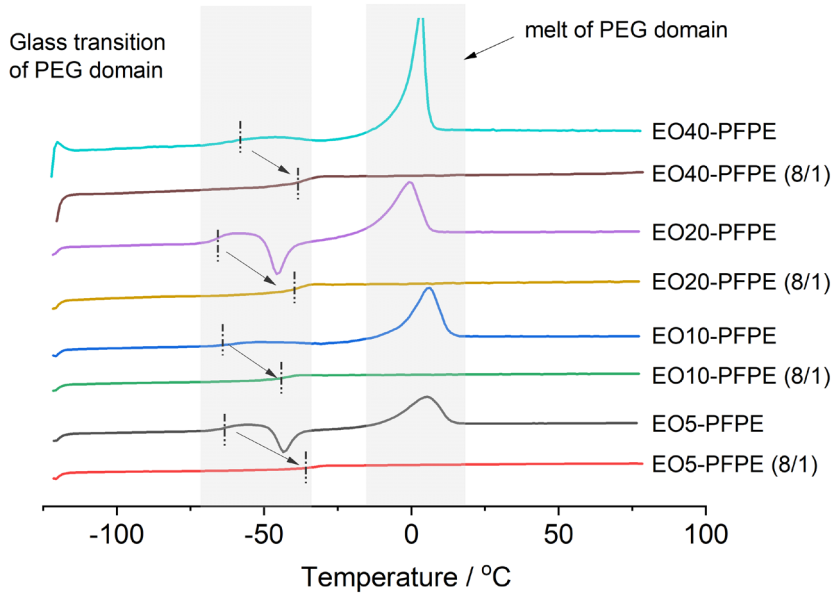

Figure S1. Tg comparison of PFPE polymers and electrolytes after adding NaFSI salts. The EO/Na^+ ratio in electrolyte is 8 to 1 as indicated in the brackets. The highlighted regions represent the glass transition (T_g) of PEG domain (left) and melt of PEG domains (right). The highlighted vertical dash lines represent the glass transition temperature (mid-point) of PEG segments.

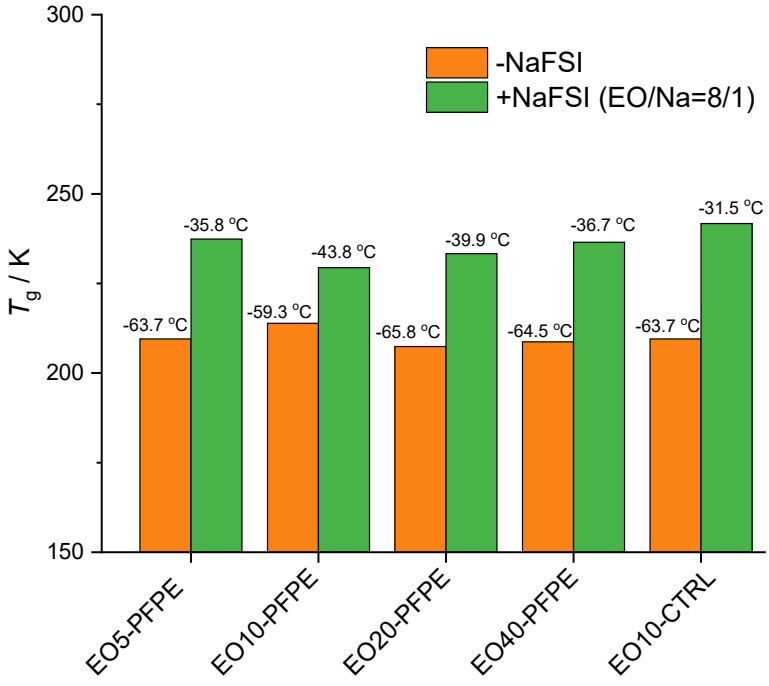

Figure S2. The extracted T_g, T_m of different polymers and related electrolytes. The EO/Na ratio of polymer electrolytes is 8:1.

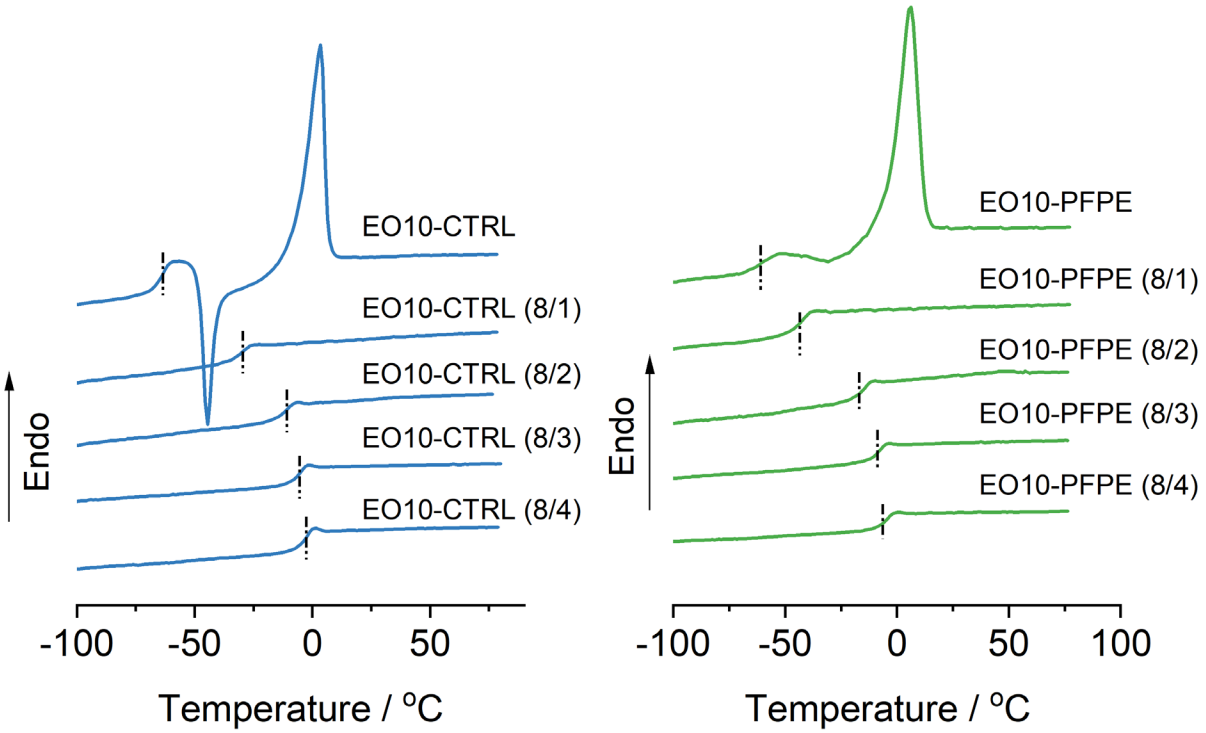

Figure S3. The DSC traces of (a) neat PFPE10 polymer and their electrolytes with different EO/Na^+ ratios, and (b) control polymer (CTRL10) and their electrolytes with different EO/Na^+ ratios The highlighted vertical dash lines represent the glass transition temperature (mid-point).

Table S2. The extract T_g values of PFPE polymer electrolytes and control electrolytes based on Figure S3.

	EO/Na =8/0	EO/Na =8/1	EO/Na =8/2	EO/Na =8/3	EO/Na =8/4
EO-PFPE	-59.3 ºC	-43.8 ºC	-15.9 ºC	-9.2 ºC	-6.8 ºC
EO-CTRL	-63.7 ºC	-31.5 ºC	-11.6 ºC	-6.7 ºC	-3.8 ºC

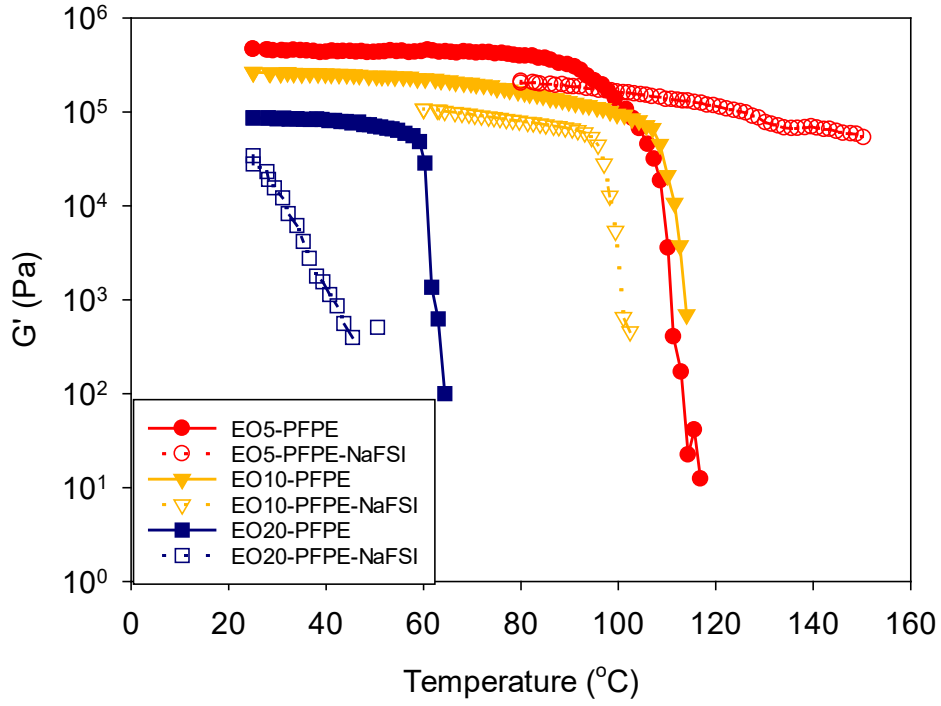

Figure S4. Rheology data showing the changes of storage modulus (G') as function of temperature. The EOm-PFPE polymers and electrolytes are compared.

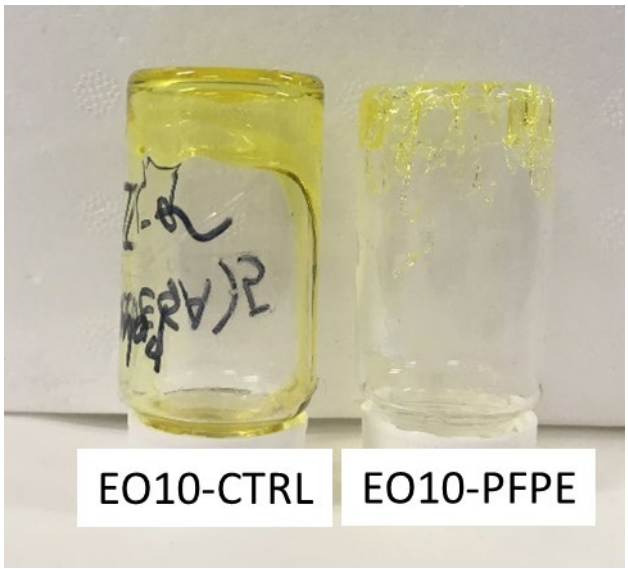

Figure S5. Digital photos of EO10-CTRL and EO10-PFPE electrolytes at room temperature. The EO10-CTRL is a viscous fluid while the EO10-PFPE is a soft solid material.

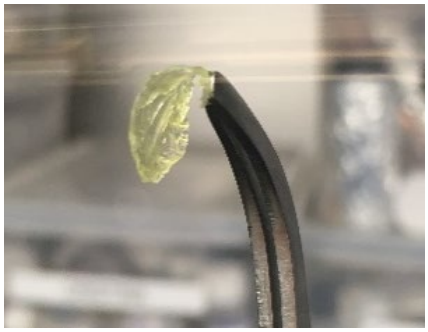

Figure S6. Digital photo of EO10-CTRL PVDF composite.

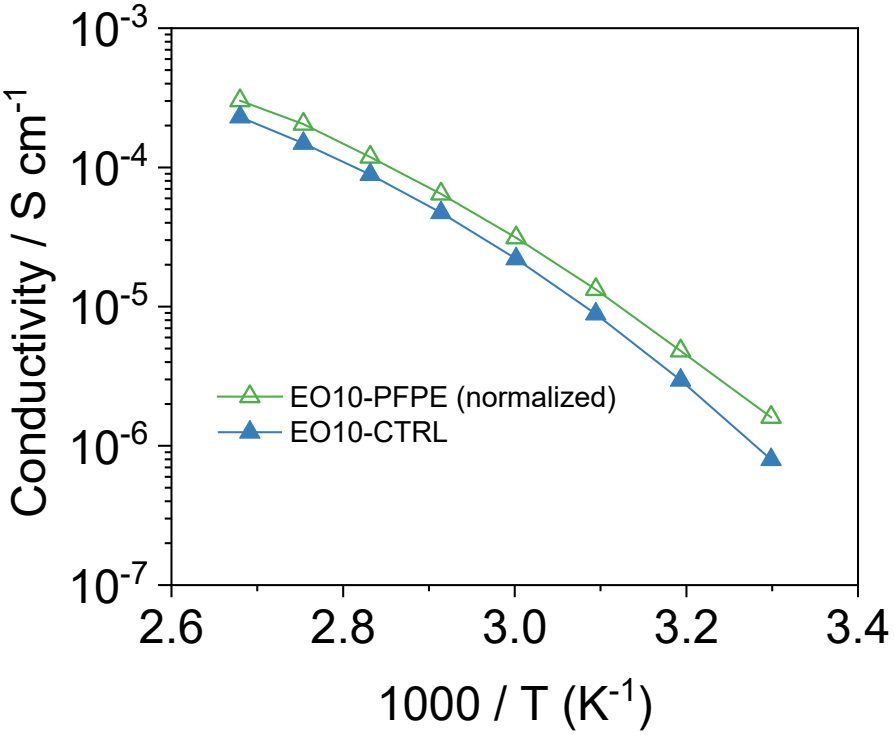

Figure S7. Comparison of normalized conductivity of EO10-PFPE and conductivity of EO10-CTRL. The normalized conductivity is calculated based on the volume fraction of PEG phase in EO10-PFPE polymer as reported in Table S1.

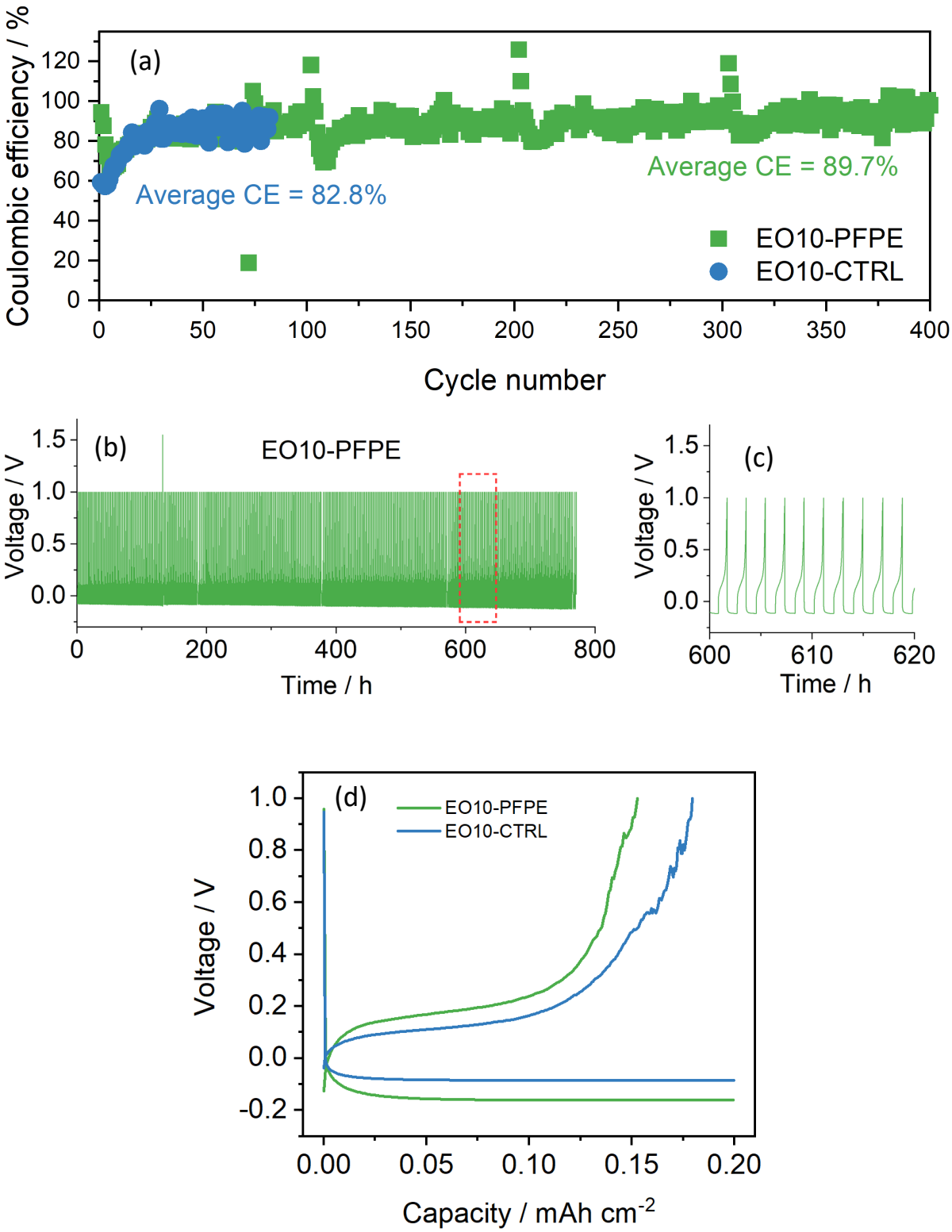

Figure S8. Coulombic efficiency (CE) of Na plating/stripping in Na/Cu cells. (a) Columbic efficiencies of Na/Cu cells with different electrolytes. (b) Voltage-time profile of Na plating/stripping with EO10-PFPE electrolyte. (c) Enlarged view of voltage profile during 600-620 h of (b). (d) The comparison of voltage profiles of Na plating and stripping processes at selected cycle of 50. For each cycle, the experiments were done by plating 0.2 mAh cm^{-2} of Na

on Cu electrode (1 hour with current density of 0.2 mA cm^{-2}) then stripping at a current density of 0.1 mA cm-2 to a cut-off voltage of 1.0 V. All experiments were done at 80 ºC

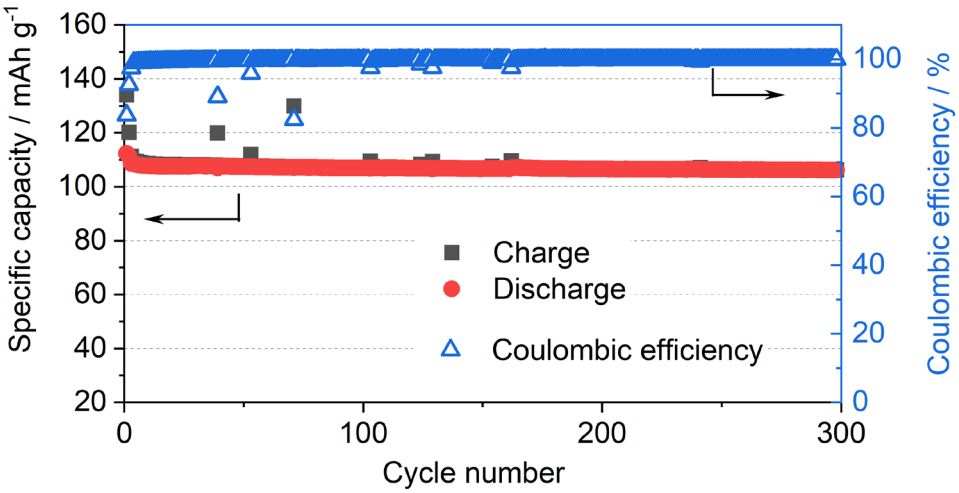

Figure S9. Long term cycling performance of Na/PFPE10-2Na/NaVP cell cycled at C/2 (80 ºC)

MD simulation methods

Initial polymer structures

In the simulations, we used the EO5-PFPE and EO5-CTRL polymers, which were of the analogous structures to the original EO10-PFPE and EO10-CTRL. The only difference between them is the number of oligoethylene glycol (EO) side chains, i.e., the polymers investigated herein had 5 EO chains containing 8 -CH_2CH_2O- units each, instead of 10 EO chains like in the EO10-PFPE and EO10-CTRL employed in the experimental part. This modification was conceived in order to enhance the polymer flexibility in the MD simulations by decreasing the size of the molecule and the level of branched chains. Hence, it resulted in a better reorganization of polymer chains, and thus, provided more reliable results after system equilibration. Since the EO5-PFPE polymer retained its amphiphilic character due to the presence of both hydrophobic fluorinated chain and polar ethylene glycol moieties, we assumed that the partial decrease in the number of EO chains would not significantly influence its properties in the simulations.

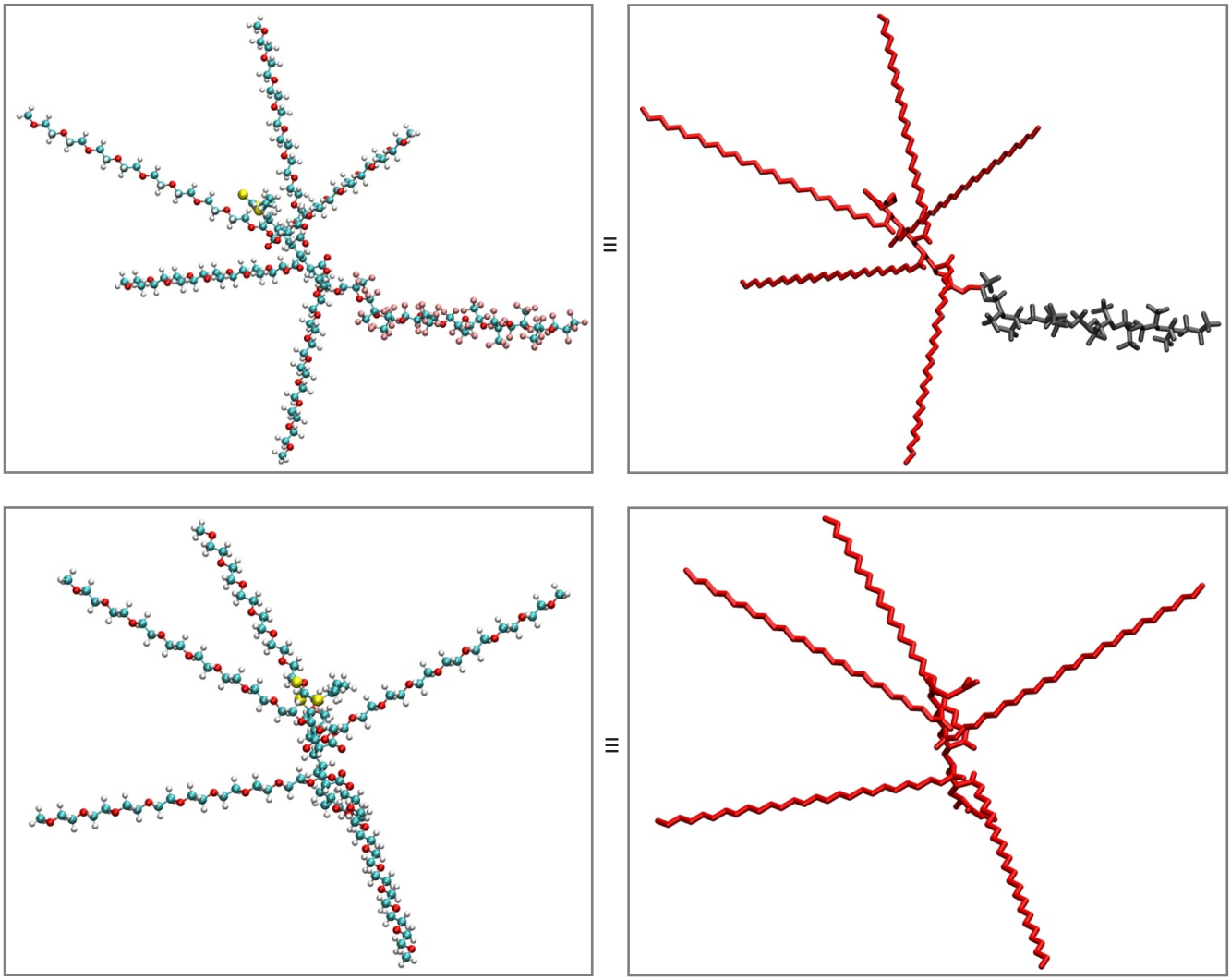

Figure S10. Chemical structures and models of EO5-PFPE and EO5-CTRL polymers studied in MD simulations. Atoms are colored as follows: C = blue, H = white, O = red, S = yellow, F = pink.

Formation of polymer-NaFSI complexes

To understand how Na^+ and FSI^- ions interact with the polymer, we started with MD simulations of the one fluorinated EO5-PFPE molecule mixed with randomly distributed 5 Na^+ and 5 FSI^- ions. The molecules were placed in a 5 × 5 × 5 nm box in vacuum, and the EO-to-Na^+ ratio was equal to 8:1. Within the first nanoseconds of simulation time, we found that Na^+ cations were rapidly captured by folding EO moieties. Figure S11 shows the equilibrated structure obtained after 600 ns. Analogously to the structure of crown ether–metal cation complexes, one Na^+ ion was surrounded by 3 to 5 oxygen atoms.

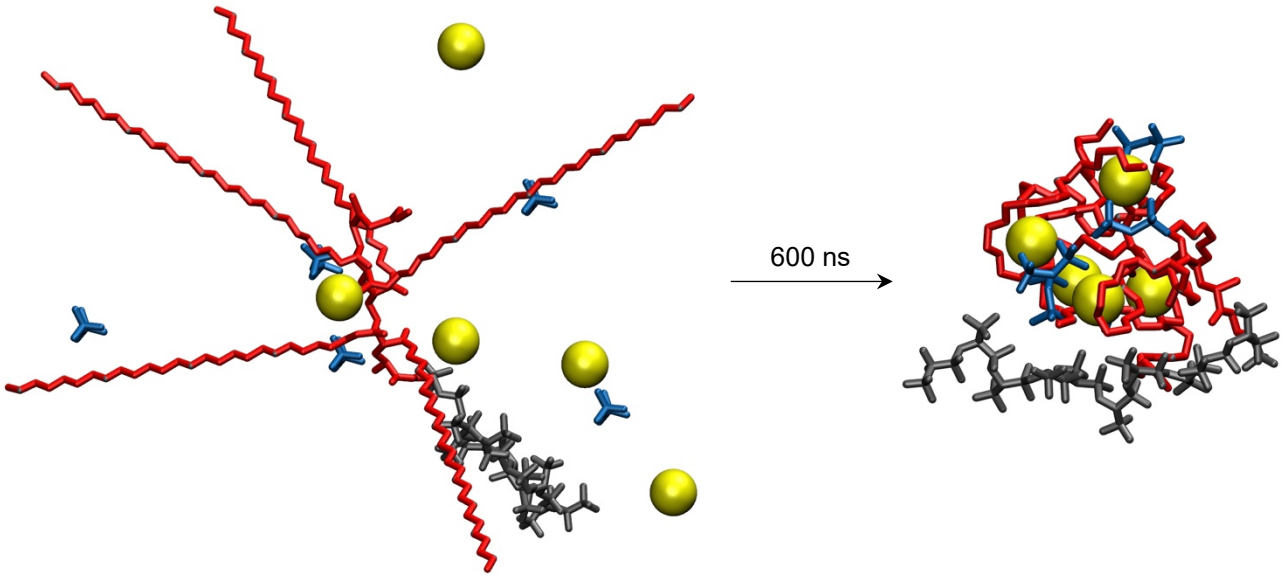

Figure S11. MD simulation of EO5-PFPE polymer with Na^+ and FSI^- ions. Na^+ = yellow spheres; FSI^- = blue; polymer backbone = red lines; fluorinated fragment of the polymer = grey lines. For clarity, hydrogen atoms are not displayed.

MD simulations in the organic solvent droplet

We ran the MD simulations for 200 ns at T = 25°C. During the first ~5 ns, the part of ether molecules spread out evenly in the box to form a gas phase, and the polymer/NaFSI solution shrank to form a spherical droplet (Figure S12). These two phases reside in equilibrium during the entire simulation. As previously, we observed Na^+ cations being captured by folded EO moieties. Analogously to the structure of crown ether–metal cation complexes, one Na^+ ion was surrounded by 3 (partial screening by FSI) to 5 (complex fully surrounded by EO units) oxygen atoms.

From the initial 1987 ether molecules in the droplet, 1405 and 1637 evaporated to form a gas phase in case (i) and (ii), respectively. Thus, the final polymer concentrations in the droplet were similar and equalled to 53.2% (i) and 55.2% (ii). Importantly, nearly all the remaining ether units have formed an external layer coating the core composed of polymer and ions. Therefore, we assumed that the interaction between ether and substantial components did not influence the reorganization processes occuring inside the core (Figure S13).

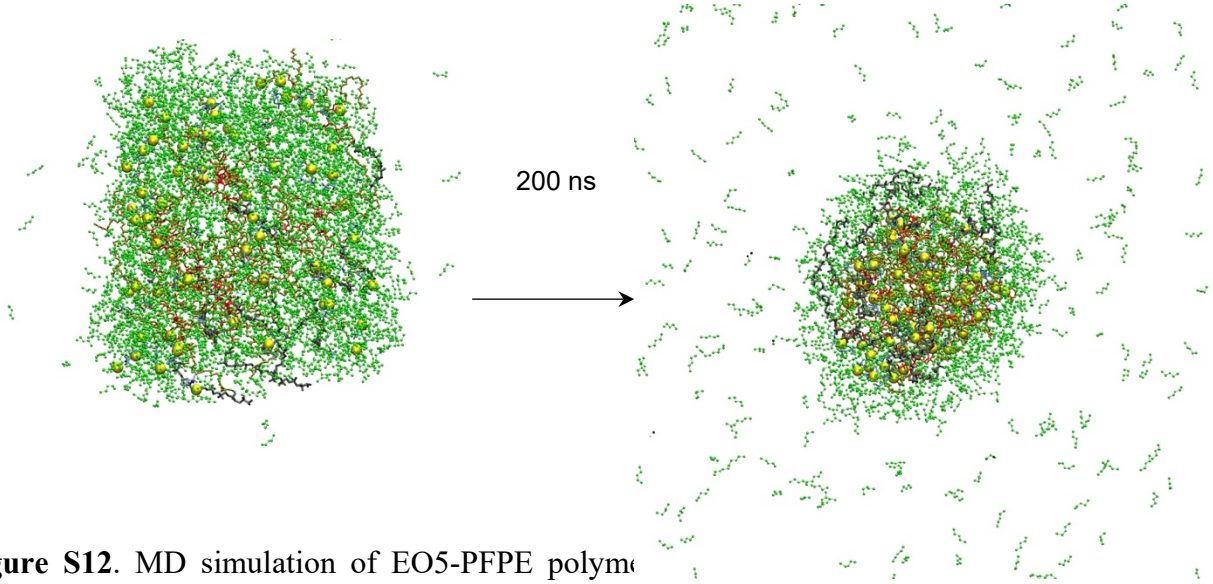

Figure S12. MD simulation of EO5-PFPE polym correspond to 0 ns and 200 ns simulation time, respectively. Na^+ = yellow spheres; FSI^- = blue; EO chains = red; fluorinated fragment of the polymer = grey; diethyl ether = green. Hydrogen atoms are hidden for clarity.

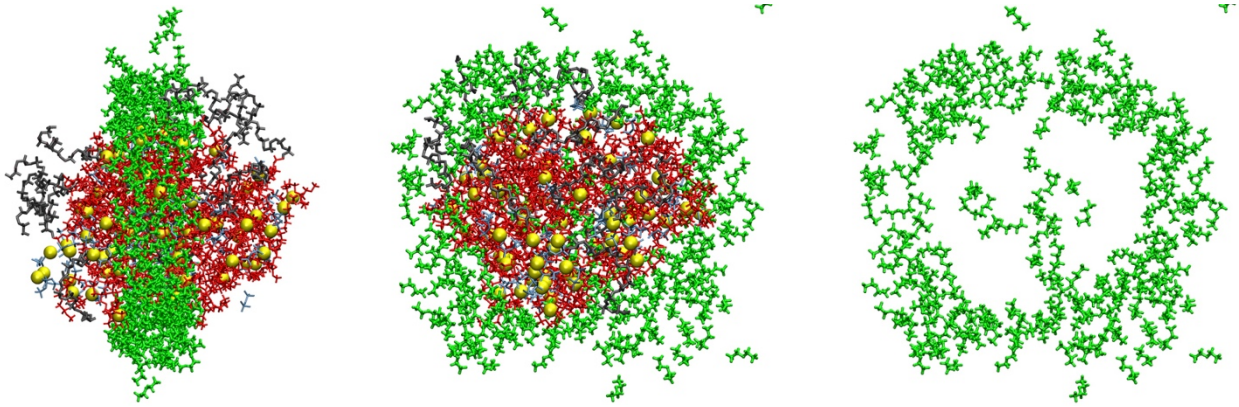

Figure S13. Cross-section of a droplet from the MD simulation including EO5-PFPE (i). Ether molecules form an external solvating layer without significant contribution to the ion/polymer internal phase. Snapshots were taken at t = 200 ns. Herein, ether cross-section along the (x,y) plane is 1.5 nm thick. Na^+ = yellow spheres; FSI^- = light blue; EO chains = red; fluorinated fragment of the polymer = grey; ether = green.

Binding energy calculations

Since the diethyl ether concentration inside of the polymer matrix was very low, for Na^+-to-polymer and FSI-to-polymer energies we used the dielectric constant of vacuum. The dielectric constant of ether at the similar temperatures and at the concentrations close to those of a gas phase, remains around 1.01 or below,[1] what makes this influence negligible, comparing to $\varepsilon = 1.00$ for vacuum.

To calculate the binding energies between the Na^+ and FSI anions, we had to include the dielectric constant of the polymer occupying the space between the ions. Similarly to the previously reported attempts where the combination of fluorinated chain with EG units for the construction of batteries has been conceived,[2] we used the dielectric constant of dimethyl-terminated oligo(ethylene glycol), $\varepsilon_{EO} = 7.2$ and for ester-terminated PFPE, $\varepsilon_{PFPE} = 3.7$.[3,4] Thus, regarding the contribution of PFPE chains and EO moieties, the approximate dielectric constant of EO5-PFPE was 6.6. Figure S15 shows the binding energies calculated in the equilibrated systems (i) and (ii) at every 10 ps.

Finally, we ran the MD simulation of the expanded system comprising eight times more of EO5-PFPE molecules with the same EO-to-Na^+ ratio, 8:1 (Figure S14). This was carried out to verify that the formation of PFPE-rich phases was not governed by the presence of ether on the surface, but rather due to the van der Waals (vdW) attraction between hydrophobic units. After calculating the binding energies in that system, we found that the expansion of the box size not only resulted in the previous trend in energy differences but emphasized the parallel formation of hydrophobic and ion-rich phases independently on each other, which had a dramatic influence on the interaction energies. Therefore, the Na^+-to-polymer (EO5-PFPE) binding energy was even smaller than in the droplet (–57.1 kcal/mol *vs*. –79.4 kcal/mol). Similarly, FSI-to-polymer binding was significantly stronger in the bulk system as well (–20.5 kcal/mol vs. –14.6 kcal/mol). All of these observations support the experimental data where the presence of hydrophobic fluorinated chains enhances the electrolyte performance (e.g. conductivity, transference number) by increasing the lability of Na^+ and binding of FSI anions by the PFPE-functionalize polymer.

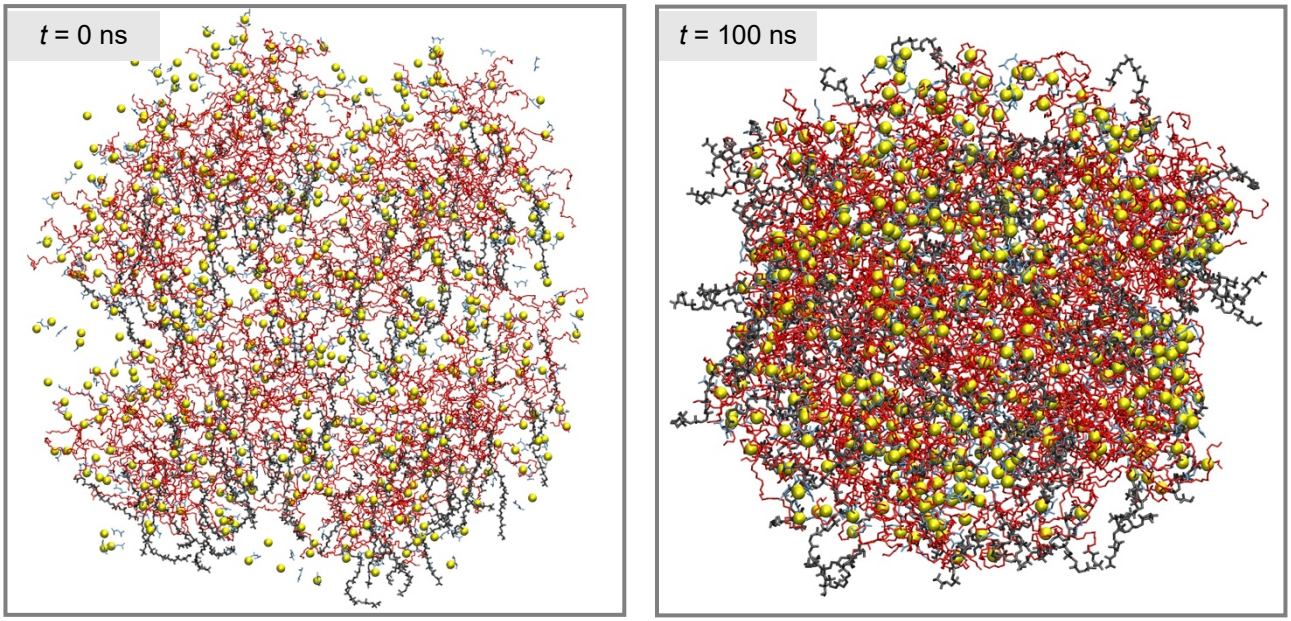

Figure S14. Morphology of the system (i) expanded eightfold at different simulation times. Na^+ = yellow spheres; FSI^- = blue; EO chains = red; fluorinated fragment of the polymer = grey. Ether molecules are hidden for clarity.

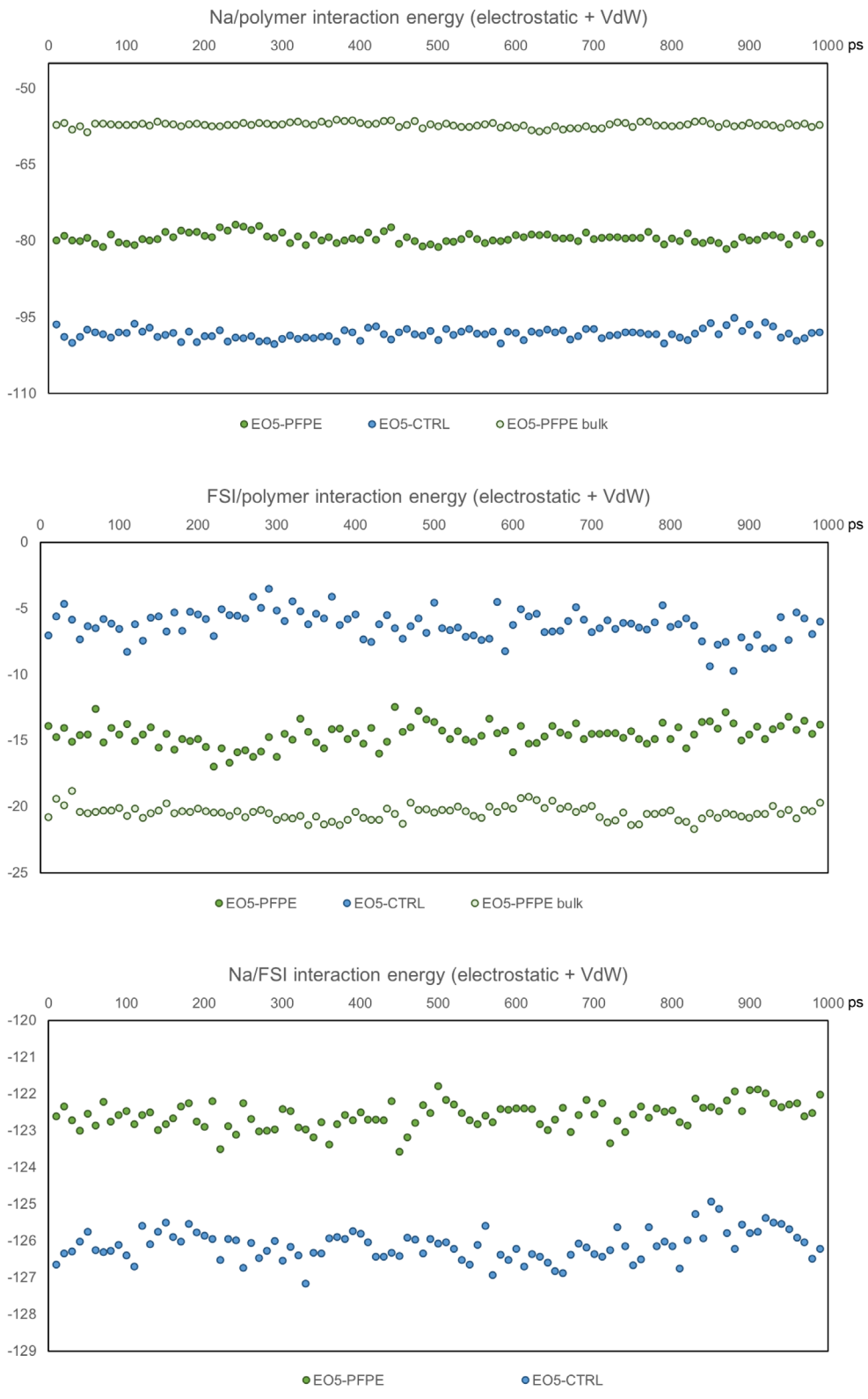

Figure S15. Energies (kcal/mol) calculated for the last 1 ns of 200 ns simulation, normalized per 1 mole of ions.

Table S3. Comparison of full cell performance with different electrolytes, electrodes and test conditions

Electrolytes	Cathode	Active material mass loading (mg cm^{-2})	Temperature (^oC)	C-rate	Initial capacity (mAh g^{-1})	Capacity retention (%)	Cycle number	Ref.
C2mpyrFSI-NaFSI/PVDF gel	$NaFePO_4$	1.0	50	0.2C	119	97.5	40	ref[5]
POSS-4PEG2K(NaE16)	δ-NaxV_2O_5	0.2	80	<0.25C	152	49	50	ref[6]
PEO-$Na_xZn_2TeO_6$	$Na_3V_2(PO_4)_3$	2.0	80	0.2	106	99.3	100	ref[7]
PFAS-Na/$NaClO_4$ carbonate liquid	Prussian Blue (HQ-NaFe)	NA	NA	1C	128	73.3	1100	ref[8]
$Na_3Zr_2(Si_2PO_{12})$ + Succinonitrile and $NaClO_4$	$Na_3V_2(PO_4)_3$	3.0	50	1C	112	98.2	100	ref[9]
PEO-NaFSI-1%Al_2O_3	$Na_3V_2(PO_4)_3$	3.0	80	1C	90	92.7	2000	ref[10]
star-like hyperbranched *β*-cyclodextrin	$NaNi_{1/3}Fe_{1/3}Mn_{1/3}O_2$	NA	60	0.1	102	88.2	80	ref[11]
Succinonitrile-polymer electrolyte	$NaNi_{1/3}Fe_{1/3}Mn_{1/3}O_2$	1.5 ~2.0	23	0.1C	105	80.0	120	ref[12]
PEGDMA-NaFSI	$Na_3V_2(PO_4)_3$	1.9	60	0.5	108	NA	926	ref[13]
PCL–PTMC-NaFSI	$NaCu_{1/9}Ni_{2/9}Fe_{1/3}Mn_{1/3}O$	1.8	80	1C	105	81.9	150	ref[14]
PEO/NaClO4/Al2O3	$Na_3V_2(PO_4)_3$	0.96	80	2C	96	87.5	1000	ref[15]
PEO/NaClO4/TiO2	$Na_{2/3}Co_{2/3}Mn_{1/3}O$	NA	60	0.1C	49	91.8	25	ref[16]
PEO-based CQDs	$Na_3V_2(PO_4)_3$	2.1	60	1C	101.5	88.6	100	ref[17]
PEO-NaPF6	$Na_3V_2(PO_4)_3$	3.0	80	2C	95	85.8	200	ref[18]
Na3Zr2Si2PO12(NZSP)/ PVDF-HFP composite	$Na_3V_2(PO_4)_3$	NA	60	0.5C	91	82.4	100	ref[19]
PEO-Na3Zr2Si2PO12	$Na_2MnFe(CN)_6$	3.0	60	NA	109.3	83.1	300	ref[20]
EO10-PFPE composite	$Na_3V_2(PO_4)_3$	1.0	80	2C	87.2	97.5	940	**This work**

References

1. W. Eltringham and O. J. Catchpole, *Journal of Chemical & Engineering Data*, 2007, **52**, 363-367.
2. K. R. Olson, D. H. C. Wong, M. Chintapalli, K. Timachova, R. Janusziewicz, W. F. M. Daniel, S. Mecham, S. Sheiko, N. P. Balsara and J. M. DeSimone, *Polymer*, 2016, **100**, 126-133.
3. C. Tonelli, P. Gavezotti and E. Strepparola, *Journal of Fluorine Chemistry*, 1999, **95**, 51-70.
4. H. Zhang, O. Arcelus and J. Carrasco, *Electrochimica Acta*, 2018, **280**, 290-299.
5. S. Malunavar, X. Wang, F. Makhlooghiazad, M. Armand, M. G. Mestres, P. Howlett and M. Forsyth, *Journal of Physics: Materials*, 2021, **submitted**.
6. Y. Zheng, Q. Pan, M. Clites, B. W. Byles, E. Pomerantseva and C. Y. Li, *Advanced Energy Materials*, 2018, **8**, 1801885.
7. J.-F. Wu, Z.-Y. Yu, Q. Wang and X. Guo, *Energy Storage Materials*, 2020, **24**, 467-471.
8. G. Du, M. Tao, J. Li, T. Yang, W. Gao, J. Deng, Y. Qi, S.-J. Bao and M. Xu, *Advanced Energy Materials*, 2020, **10**, 1903351.
9. H. Gao, L. Xue, S. Xin, K. Park and J. B. Goodenough, *Angewandte Chemie*, 2017, **129**, 5633-5637.
10. L. Liu, X. Qi, S. Yin, Q. Zhang, X. Liu, L. Suo, H. Li, L. Chen and Y.-S. Hu, *ACS Energy Letters*, 2019, **4**, 1650-1657.
11. S. Chen, F. Feng, Y. Yin, H. Che, X.-Z. Liao and Z.-F. Ma, *Journal of Power Sources*, 2018, **399**, 363-371.
12. S. Chen, F. Feng, Y. Yin, X. Lizo and Z. Ma, *Energy Storage Materials*, 2019, **22**, 57-65.
13. Y. Yao, Z. Wei, H. Wang, H. Huang, Y. Jiang, X. Wu, X. Yao, Z.-S. Wu and Y. Yu, *Advanced Energy Materials*, 2020, **10**, 1903698.
14. Q. Ma, J. Liu, X. Qi, X. Rong, Y. Shao, W. Feng, J. Nie, Y.-S. Hu, H. Li, X. Huang, L. Chen and Z. Zhou, *Journal of Materials Chemistry A*, 2017, **5**, 7738-7743.
15. R. Gao, R. Tan, L. Han, Y. Zhao, Z. Wang, L. Yang and F. Pan, *Journal of Materials Chemistry A*, 2017, **5**, 5273-5277.
16. Y. L. Ni'mah, M.-Y. Cheng, J. H. Cheng, J. Rick and B.-J. Hwang, *Journal of Power Sources*, 2015, **278**, 375-381.
17. C. Ma, K. Dai, H. Hou, X. Ji, L. Chen, D. G. Ivey and W. Wei, *Advanced Science*, 2018, **5**, 1700996.
18. Q. Zhang, Y. Lu, H. Yu, G. Yang, Q. Liu, Z. Wang, L. Chen and Y.-S. Hu, *Journal of The Electrochemical Society*, 2020, **167**, 070523.
19. W. Ling, N. Fu, J. Yue, X.-X. Zeng, Q. Ma, Q. Deng, Y. Xiao, L.-J. Wan, Y.-G. Guo and X.-W. Wu, *Advanced Energy Materials*, 2020, **10**, 1903966.
20. X. Yu, L. Xue, J. B. Goodenough and A. Manthiram, *ACS Materials Letters*, 2019, **1**, 132-138.